Colloquium: Aligning molecules with strong laser pulses

Henrik Stapelfeldt

Department of Chemistry, University of Århus, DK-8000 Århus C, Denmark

Tamar Seideman

Steacie Institute for Molecular Sciences, National Research Council of Canada, Ottawa, Ontario K1A 0R6, Canada

(Published 17 April 2003)

We review the theoretical and experimental status of intense laser alignment—a field at the interface between intense laser physics and chemical dynamics with potential applications ranging from high harmonic generation and nanoscale processing to stereodynamics and control of chemical reactions. After placing the intense laser approach in context with other alignment techniques, we proceed with a discussion of the physics underlying this technique and a description of methods of observing it in the laboratory. The roles played by the laser frequency, the pulse duration, and the system temperature are illustrated numerically and experimentally. Alignment is extended to three-dimensional orientational control, a method of hindering the rotation about all three axes of polyatomic molecules. We conclude with a discussion of potential applications of intense laser alignment.

CONTENTS

I. INTRODUCTION

Most chemical reactions depend on the relative orientation of the reactants. In the case of bimolecular reactions, this statement is intuitively clear since molecules are, in general, not spherically symmetric objects. A well-known example of the dependence of reactivity upon the relative orientation of the reactants is the S_N2 reaction type; for instance: $Cl^- + CH_3I \rightarrow CH_3Cl + I^-$. Here the reaction rate is maximized if the Cl^- ion attacks methyliodide from the methyl group end. There are also orientational effects in unimolecular reactions. In photochemical processes, for instance, absorption of polarized light depends upon the alignment of the molecule with respect to the polarization direction. This follows directly from the symmetry selection rules. A simple example is vibrational excitation of CO_2: Excitation of the fundamental asymmetric stretch vibration is maximized if the exciting light is polarized along the molecular axis, whereas excitation of the fundamental bending vibration is maximized if the exciting light is polarized perpendicular to the molecular axis.

Development of techniques to align or orient molecules has therefore been an important goal of chemical reaction dynamics. Those techniques that define order of the molecular geometry with respect to a space fixed axis are said to create alignment. Those that also define a direction with respect to the space fixed axis, i.e., break the inversion symmetry, are said to create orientation. The techniques developed so far rely on the use of (1) collisional processes, (2) static electric fields, and (3) optical fields.

When molecules seeded in a monoatomic gas are supersonically expanded into vacuum, collisions between molecules and atoms force the rotational angular momentum to align preferentially perpendicular to the flight direction (Pullmann *et al.*, 1990; Aquilanti *et al.*, 1994, 1999; Pirani *et al.*, 2001). Thus, a sample of molecules with an anisotropy in the projection of the rotational angular momentum onto the flight direction is created, and therefore an anisotropic spatial distribution.

Based on static electric fields, two techniques are available for orientation of molecules. Within the electrical hexapole focusing technique (Brooks, McKillop, and Pippin, 1979; Stolte, 1988; Cho and Bernstein, 1991; Baugh *et al.*, 1994), an electrostatic hexapole field is used to select a single rotational state, $|JKM\rangle$. A single quantum eigenstate is generally anisotropic although, by the nature of quantum mechanics, it cannot be sharply defined in angular space. The ability of this method to produce magnetic-state-selected molecules has interesting applications (Seideman, 1995a; Torres *et al.*, 1997) but the apparatus necessary is rather elaborate.

Within the strong dc field technique (nicknamed "brute force" orientation) (Loesch and Remscheid, 1990; Friedrich and Herschbach, 1991; Wu, Bemish, and Miller, 1994), polar molecules are placed in a very strong static electric field. If the interaction energy of the mol-

ecule with the field is much larger than the rotational energy, the molecules are oriented. Since there is an upper limit to the strength of a static field that can be exerted on molecules, the brute force method is suitable for molecules that both have a large dipole moment and can be strongly rotationally cooled in a supersonic expansion.

The power of the two techniques mentioned above is that they arrange molecules in a head-versus-tail order, i.e., they orient the molecules. Their weakness is that neither is general. An alternative approach is based on the application of optical fields to align molecules. When randomly oriented molecules are irradiated by polarized light, resonant with a parallel or a perpendicular transition, the excitation probability depends upon the angle between the transition dipole vector and the polarization vector (Estler and Zare, 1978; Weida and Parmenter, 1997). As a result, a sample of aligned molecules in either a vibrationally or an electronically excited state is created. Also, alignment of ground-state molecules can be created by using the exciting light to remove (and hence leave behind), for instance, by photodissociation, an anisotropic distribution (de Vries *et al.*, 1983). The strength of the photoselection technique is that it applies to a large number of molecules and it can be used to make aligned molecules either in the ground state or in an excited state. Its weakness is that only a rather small fraction (a few percent) of molecules from the original sample is selected; in the weak-field limit, the population of the initial state is essentially unmodified by the interaction.

A different way of using optical fields to align molecules is to replace the static field in the brute force orientation method with a strong, linearly polarized laser field (Zon and Katsnel'son, 1976; Friedrich and Herschbach, 1995a, 1995b; Seideman, 1995b). As discussed in the following sections, the intense laser approach to alignment reduces in one limit to alignment in a strong dc field (Loesch and Remscheid, 1990; Friedrich and Herschbach, 1991; Wu, Bemish, and Miller, 1994) and in another to the method of optical polarization (Estler and Zare, 1978; Weida and Parmenter, 1997; de Vries *et al.*, 1983). It shares the practicality of the former and the generality of the latter. It does, however, offer unique opportunities. One new feature is the possibility of producing field-free strongly aligned molecules, illustrated in Secs. II.A.2 and III.B. For applications to stereodynamical studies and gas-surface research it is important that the aligned molecules be free of strong external fields, as such fields can modify the chemistry. A second is the possibility of extending alignment to three-dimensional (3D) orientational control, illustrated in Secs. II.B and III.C. Conventional (1D) alignment hinders the rotation about one of the three axes of a polyatomic molecule, leaving it free to rotate about one (for linear molecules) or two (for nonlinear molecules) axes. Several of the new applications proposed in Sec. IV rely on our ability to hinder the rotation in all three Euler angles of polyatomic molecules. Finally, the sharpness of the alignment attained in strong laser fields

cannot be matched by more conventional approaches. An important disadvantage of this as compared to other schemes will become apparent in the following sections, namely, orienting molecules is a much more difficult problem than aligning them in a strong laser field. Recent work addressing this challenge is discussed in Sec. V.

During the past few years the field of intense laser alignment has been growing rapidly, with an ever increasing number of contributions from both experimental (Kim and Felker, 1996, 1997; Larsen *et al.*, 1998, 1999, 2000; Sakai, Safvan, 1998; Lappas and Marangos, 2000; Baumfalk, Nahler, and Buck, 2001; Rosca-Pruna and Vrakking, 2001, 2002a, 2002b; Velotta *et al.*, 2001; Bartels *et al.*, 2002; Poulsen, Skovsen, and Stapelfeldt, 2002; Sakai *et al.*, 2002) and theoretical (Friedrich and Herschbach, 1995a, 1995b, 1999; Seideman, 1995b, 1999a, 1999b, 2001a; Sukharev and Krainov, 1998; Andryushin and Fedorov, 1999; Dion, Bandrauk, Atabek, Keller, Umeda, and Fujimura, 1999; Dion, Keller, Atabek, and Bandrauk, 1999; Henriksen, 1999; Ortigoso *et al.*, 1999; Yan and Seideman, 1999; Keller, Dion, and Atabek, 2000; Larsen *et al.*, 2000; Legare, Chelkowski, and Bandrauk, 2000; Averbukh and Arvieu, 2001; Cai, Marango, and Friedrich, 2001; Dion, Keller, and Atabek, 2001; Hoki and Fujimura, 2001; Machholm, 2001; Machholm and Henriksen, 2001; Dion *et al.*, 2002; Guerin *et al.*, 2002; Kalosha *et al.*, 2002; Van Leuven, Malvaldi, and Persico, 2002) research. Recent work has analyzed the role played by various system properties (Ortigoso *et al.*, 1999), developed a genetic algorithm to optimize strong field orientation (Auger *et al.*, 2002; Ben Haj Yedder *et al.*, 2002; Dion *et al.*, 2002), discussed the alignment of vibrationally excited states (Legare, Chelkowski, and Bandrauk, 2000), and introduced a variety of new and exciting applications of laser alignment (Seideman, 1997a, 2000, 2001b; Lappas and Marangos, 2000; Velotta *et al.*, 2001; Bartels *et al.*, 2002; Kalosha *et al.*, 2002). Several of these applications are discussed in Sec. IV. Space considerations preclude us from reviewing all or even the highlights of this work in the present Colloquium. We acknowledge here the important contributions made by a large number of scientists during the past few years and regret that the format of this Colloquium does not permit us to expand on individual contributions. We hope that the Colloquium will provide the reader with easy access to the relevant literature of interest.

Our paper is organized in the following way: In Sec. II we discuss the theory of intense laser alignment, focusing on the qualitative concepts and omitting the technical details. Section III contains a description of experimental observations of alignment. In Sec. IV we discuss several applications of laser-aligned molecules and finally a conclusion is given in Sec. V.

II. THEORY

In this section we discuss the physical origin of intense laser alignment within a quantum-mechanical framework. In order to keep the discussion as brief and trans-

parent as possible, we omit the formalism and the technical details and focus on the qualitative questions. The interested reader is referred to Seideman (1995b, 1999a, 2001a) for details of our method of computing laser alignment. We begin in Sec. II.A with the physics of conventional (1D) laser alignment. In Sec. II.B we extend the discussion to 3D alignment. Atomic units are used throughout this Colloquium.

A. One-dimensional alignment

1. Near-resonant vs nonresonant alignment

Consider a molecule subject to a linearly polarized laser field whose frequency is tuned near resonance with an electronic (or vibrational) transition. In the weak-field limit, if the system has been initially prepared in a rotational level J_0, electric dipole selection rules allow J_0 and $J_0 \pm 1$ in the excited state. The interference between these levels gives rise to a mildly aligned excited state population; the probability scales as $\cos^2 \theta$ for parallel, and as $\sin^2 \theta$ for perpendicular transitions, θ being the angle between the molecular symmetry axis and the field polarization vector.

At nonperturbative intensities, the system undergoes Rabi-type oscillations between the two resonant states, exchanging another unit of angular momentum with the field on each transition. Consequently, a rotationally broad wave packet is produced in both states. The associated alignment is considerably sharper than the $\cos^2 \theta$ or $\sin^2 \theta$ weak-field distribution, as it arises from the interference of many levels (Seideman, 1995b, 1999a).

The degree of rotational excitation is determined by either the pulse duration or the balance between the laser intensity and the detuning from resonance. In the limit of a short, intense pulse the number of levels that can be excited is, roughly speaking, the number of cycles the system has undergone between the two states, $J_{max} \sim \tau/\Omega_R^{-1}$, where τ is the pulse duration, $\Omega_R \propto \varepsilon_m$ is the Rabi coupling,[1] Ω_R^{-1} is the corresponding period, and ε_m is the field amplitude. In the case of a long, or lower intensity, pulse, J_{max} is determined by the accumulated detuning from resonance, i.e., by the requirement that the Rabi coupling be sufficient to access rotational levels that are further detuned from resonance as the excitation proceeds. In the case of a linear molecule we have $J_{max} \sim \sqrt{\varepsilon_m \mu/2B_e}$, where μ is the matrix element of the transition dipole operator in the electronic basis and B_e is the rotational constant. A quantitative discussion is given in Seideman (2001a).

Rather similar coherent rotational excitation dynamics takes place at nonresonant frequencies, well below electronic transition frequencies. In this case a rotationally broad superposition state is produced via sequential Raman-type ($|\Delta J| = 0,2$) transitions, the system remain-

ing in the ground vibronic state (Seideman, 2001a). The qualitative criteria determining the degree of rotational excitation remain the same as discussed in connection with the near-resonance case. Here, however, the Rabi coupling is proportional to the square of the field, due to the two-photon nature of the cycles. Consequently, much higher intensities are required to achieve a given degree of alignment, as expected for a nonresonant process. On the other hand, much higher intensities can be exerted at nonresonant frequencies, as undesired competing processes scale similarly with detuning from resonance.

Thus, polarized laser pulses of sufficient intensity and duration can readily populate broad rotational wave packets at either near-resonant or nonresonant frequencies. It remains, however, to investigate the conditions under which such wave packets necessarily align. In general, the excitation of a broad wave packet of eigenstates in a given mode is an essential, but not a sufficient, condition for the conjugate coordinate to be well defined. The degree of spatial localization depends on the relative phases of the wave-packet components. In the specific case of rotational wave packets, this phase relationship is determined primarily by the temporal shape of the laser pulse, as illustrated in the following subsection.

2. Adiabatic vs dynamical alignment

The simplest case scenario is that of alignment in a cw field, proposed in Friedrich and Herschbach (1995a, 1995b), where dynamical considerations play no role. In practice, intense field experiments are carried out in pulsed mode, but, provided that the pulse is long compared to the rotational periods, each eigenstate of the field-free Hamiltonian is guaranteed to evolve adiabatically into the corresponding state of the complete Hamiltonian during the turn-on, returning to the original (isotropic) field-free eigenstate upon turn-off. Formally, the problem is thus reduced to alignment in a cw field of constant amplitude ε_m. The latter problem is equivalent to alignment of nonpolar molecules in a strong dc field, since the rapid oscillations of the ac field can be eliminated at both near-resonance and nonresonance frequencies (Seideman, 1995b, 2001a). Thus, in the long pulse limit, $\tau \gg \tau_{rot}$, laser alignment reduces to an intensively studied problem that is readily understood in classical terms, namely, the problem of field-induced pendular states (Loesch and Remscheid, 1990; Friedrich and Herschbach, 1991, 1995a, 1995b). In this limit, the sole requirement for alignment is that the Rabi coupling (cf. footnote 1) be large as compared to the rotational energy of the molecules.

Adiabatic alignment of I_2 molecules, calculated by exact solution of the time-dependent Schrödinger equation (see Seideman, 1995b, 2001a) is illustrated in Fig. 1. The nonresonant alignment field is linearly polarized, with a peak intensity of 10^{12} W cm^{-2} and a Gaussian envelope of duration $\tau = 3.5$ ns. Panel (a) shows the probability density as a function of time and the polar Euler angle θ

---

[1]The Rabi coupling, conventionally denoted Ω_R, is the matrix element of the field matter interaction in the rovibronic basis. It is proportional to ε_m at near-resonant and to ε_m^2 at nonresonant frequencies.
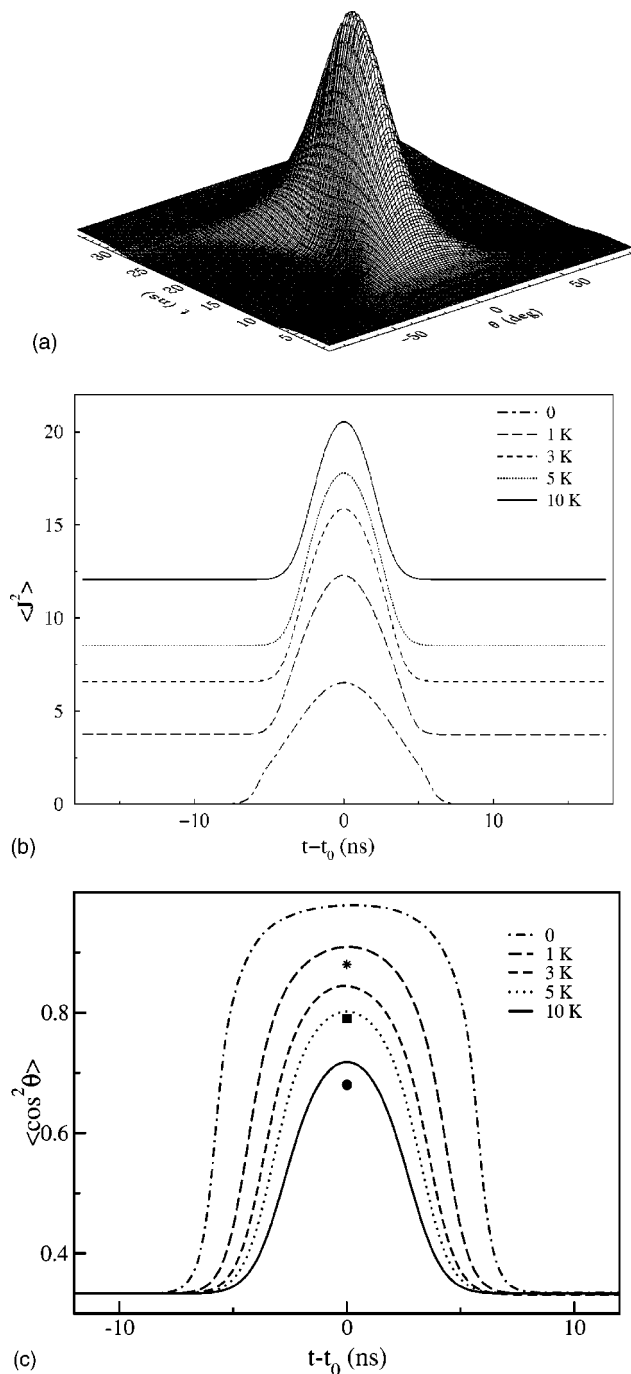
(a)

(b)

(c)

FIG. 1. Alignment of I_2 molecules under adiabatic ($\tau > \tau_{rot}$) conditions. (a) The probability density vs time and the angle between the polarization and the internuclear axes. (b) The expectation value of the squared angular momentum in the wave packet. (c) The expectation value of $\cos^2 \theta$ in the wave packet. The rotational temperature in panels (b) and (c) is 0 K (dot-dashed curves); 1 K (long-dashed curves); 3 K (dashed curves); 5 K (dotted curves); and 10 K (solid curves). The intensity is 10^{12} W cm^{-2} and the pulse duration is 3.5 ns. The symbols in panel (c) show experimentally measured values of $\langle \cos^2 \theta \rangle$ where the rotational temperature is varied by changing the buffer gas: 4 bar He (stars); 1 bar Ar (squares); 1 bar He (circles).

between the polarization and the molecular axes. As the interaction adiabatically switches on, the free rotor transforms into an eigenstate of the complete Hamiltonian, a so-called pendular state that librates about the polarization axis. Upon adiabatic turn-off the librator returns to the isotropic free rotor from which it originated. Panels (b) and (c) show the expectation values of the total angular momentum and of $\cos^2 \theta$ in the time-evolving wave packet, providing average measures of the degrees of rotational excitation and the consequent alignment, respectively. The rotational temperature in Figs. 1(b) and 1(c) increases from 0 to 10 K. Superimposed on Fig. 1(c) are experimental values of $\cos^2 \theta$, measured for I_2 molecules supersonically expanded in either argon or helium, and subjected to a laser field of peak intensity 10^{12} W cm^{-2} and pulse duration of 3.5 ns. Our method of measuring the data shown in Fig. 1(c) is detailed in Sec. III.A.

I_2 is a heavy molecule with a relatively large polarizability anisotropy. Hence a broad wave packet of rotations [see Fig. 1(b)] corresponding to remarkably sharp alignment is attained at moderate intensity. The large mass translates also into the requirement of long pulses, $\tau > \tau_{rot} = \pi / B_e$. Less polarizable molecules require higher intensities to attain similar alignment. Since, however, nonresonant ionization rates scale as the polarizability, less polarizable molecules can generally withstand higher intensities. Lighter molecules also require higher intensities to attain the sharp alignment of Fig. 1, but shorter pulses suffice and hence the pulse energy and the risk of nonresonant ionization remain comparable.

Figure 1 illustrates both the beauty and the limitation of adiabatic laser alignment; clearly the alignment is lost once the laser pulse is turned off. Theoretical studies (Seideman, 1995b, 1999a, 2001a; Dion, Keller, *et al.*, 1999; Ortigoso *et al.*, 1999; Yan and Seideman, 1999; Keller, Dion, and Atabek, 2000) have illustrated early on the possibility of retaining the field-induced alignment after turn-off of the laser pulse, through nonadiabatic rotational excitation. A short laser pulse, $\tau < \tau_{rot}$, leaves the system in a coherent superposition of rotations that is aligned upon turn-off, dephases at a rate proportional to the square of the wave-packet width in J space, and subsequently revives and dephases periodically in time. As long as coherence is maintained, the alignment is reconstructed at predetermined times and survives for a perfectly controllable period. Interestingly, under rather general conditions, the alignment is significantly enhanced after turn-off of the laser pulse (Seideman, 1999a). The origin of the phenomenon of enhanced field-free alignment is unraveled in Seideman (1999a) by means of an analytical model of the revival structure of rotational wave packets. Here, we limit attention to a numerical illustration supplemented by hand-waving arguments.

Figure 2 gives the expectation values of J and $\cos^2 \theta$ in a time-evolving wave packet during and subsequent to a laser pulse of time duration varying from the ground-state rotational period, $\tau_{rot} = \pi / B_e$, to a small fraction of
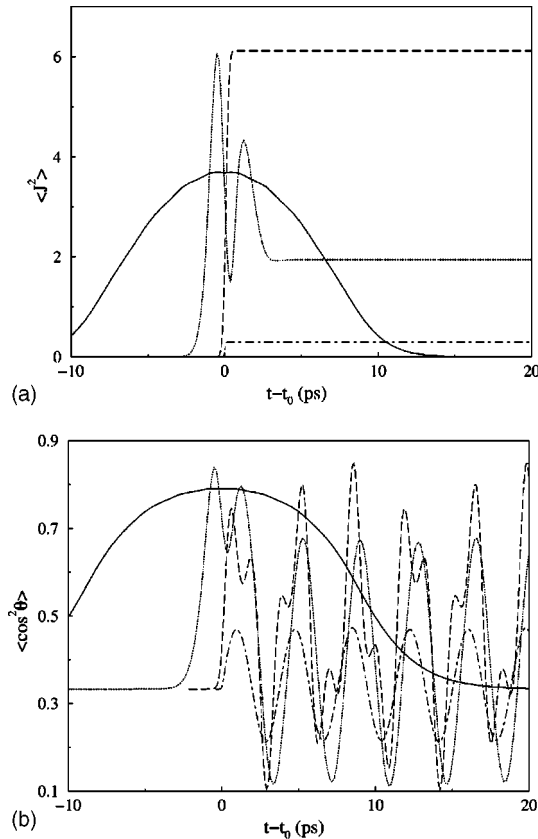
(a)

(b)

FIG. 2. Alignment of HCN molecules under nonadiabatic ($\tau < \tau_{\rm rot}$) conditions. The intensity is $5 \times 10^{12}\,\mathrm{W\,cm^{-2}}$. (a) The expectation value of the squared angular momentum in the wave packet. (b) The expectation value of $\cos^2 \theta$ in the wave packet. $\tau = \tau_{\rm rot} = \pi/B_e$ (solid curve); $\tau = \tau_{\rm rot}/5$ (dotted curve); $\tau = \tau_{\rm rot}/25$ (dashed curve); $\tau = \tau_{\rm rot}/125$ (dot-dashed curve).

$\tau_{\rm rot}$. To complement the results of Fig. 1, we consider HCN, a light molecule of low polarizability anisotropy, which has been studied numerically before (Keller, Dion, and Atabek, 2000) and is relevant to one of the applications discussed in Sec. IV. At $\tau = \tau_{\rm rot}$ (solid curve), the alignment is essentially adiabatic, the system returning to the isotropic state by the end of the pulse. With $\tau = \tau_{\rm rot}/5$ (dotted curve) the alignment is not lost upon turn-off but part of the population has returned to low rotational levels [Fig. 2(a)] and hence the field-free alignment is well below the alignment attained in the field. The dashed curve, corresponding to $\tau = \tau_{\rm rot}/25$, illustrates the phenomenon of enhanced alignment after the turn-off. Similar results are obtained for a wide range of pulse durations, although the sharpening of the alignment as compared to the adiabatic limit is characteristic of a relatively narrow τ range. Finally, with $\tau = \tau_{\rm rot}/125$ (dot-dashed curve), the pulse duration allows too few cycles for significant alignment to result at the considered intensity. A higher intensity would be required to decrease the Rabi period $\Omega_R^{-1} \propto \varepsilon_m^2$ to below τ, thus restoring the rotational excitation and the associated alignment. In the case of linear molecules and linear polarization the time-dependent Schrödinger equation can be readily expressed in reduced units where

system parameters are scaled out (Seideman, 1995b; Ortigoso *et al.*, 1999). It follows that, similar to the results of Fig. 1, those of Fig. 2 are general. Only the intensity and the pulse duration required to obtain a given time evolution of the alignment are system dependent.

The ultrashort pulse limit of enhanced alignment, where the interaction is an impulse as compared to rotations, is again readily understood in classical terms (Seideman, 1999a). In this limit an intense pulse imparts a "kick" to the molecule that rapidly transfers a large amount of angular momentum to the system and gives rise to alignment that sets in only after the turn-off. We note that gas-phase femtochemistry experiments are often carried out under conditions close to the impulse limit. High intensities are difficult to avoid in ultrafast pump-probe spectroscopy experiments. For relatively heavy systems the pump pulse is thus instantaneous on the rotational time scale, $\tau \ll \tau_{\rm rot}$, but sufficiently long to coherently excite rotations, $\tau > \Omega_R^{-1}$ (recall that $\Omega_R \propto \varepsilon_m$ in the near-resonance case). The molecule is rotationally frozen during the interaction but the sudden "kick" is encoded in the wave packet's rotational composition and gives rise to alignment after the pulse turn-off.

Thus, in both the long, $\tau > \tau_{\rm rot}$, and the ultrashort, $\tau \ll \tau_{\rm rot}$, pulse limits intense laser alignment is readily understood in classical terms, at least on a qualitative level. We show elsewhere that both limits allow for an analytical solution, hence offering useful insight (Seideman, 2001a). The intermediate pulse-length case is not amenable to analytical formulation but offers control over the alignment dynamics through choice of the field parameters.

A third mode of alignment is introduced in Yan and Seideman (1999) in the context of simultaneous alignment and focusing of molecular beams, potentially a route to nanoscale surface processing (Seideman, 1997a). To that end the combination of a long turn-on with a rapid turn-off is necessary,

$$\varepsilon(t) \propto \{1 + e^{(t_0 - t)/\tau_{\rm on}} + e^{(t-t_0)/\tau_{\rm off}}\}^{-1}, \quad \tau_{\rm on} > \tau_{\rm rot}, \tau_{\rm off} \ll \tau_{\rm rot}. \tag{1}$$

A rotational eigenstate subject to a pulse of the form (1) evolves during the turn-on into an eigenstate of the complete Hamiltonian—an aligned many-J hybrid—as in the long-pulse limit. Upon rapid turn-off the wave packet components are phased together to make the full Hamiltonian eigenstate but now evolve subject to the field-free Hamiltonian. The wave packet dephases at a rate determined by the intensity and subsequently revives. At each multiple of the rotational revival time, $t = t_0 + n\,\pi/B_e$, the alignment attained at the pulse peak is precisely reconstructed.[2] At half revival times, $t = t_0 + (n + \frac{1}{2})\pi/B_e$, the molecule aligns perpendicular to the field. Elsewhere the wave packet is nearly but not quite isotropic, cf. Fig. 2(c). The rotational components have fully dephased and hence the sharp alignment that relies

---

[2]A first experiment along these lines has now been performed (Stolow, 2002).

on a specific phase relationship is lost. Nevertheless mild alignment, arising from the natural anisotropy of the wave-packet components, survives. Illustrations of the alignment resulting from a pulse of the form (1) and a discussion of potential applications of this alignment are given in Seideman (2001a).

B. Three-dimensional alignment

As discussed in the previous section, a linearly polarized pulse of sufficient duration and intensity produces a broad wave packet of J levels. Under rather general conditions, such wave packets are tightly aligned; the polar Euler angle θ is confined to a smaller range the broader the wave packet in J space. Nonetheless, the projection of J onto the field polarization direction—the magnetic quantum number M—is conserved in a linearly polarized field and hence the molecule remains free to rotate about the polarization vector. The projection of J onto the molecular axis (K) is either rigorously conserved (as, e.g., in a field tuned near resonance with a parallel transition) or changes by only one or two quanta (as, e.g., in a field tuned near resonance with a perpendicular transition or a nonresonant field interacting with an asymmetric top molecule). Thus, the rotation about the molecular axis remains free or essentially free. Similarly, a circularly polarized intense pulse excites a broad superposition of J levels but cannot produce a wave packet in either M or K space; the molecule is confined to a plane but within this plane it is free to rotate.

In this section we show that an elliptically polarized intense field can eliminate the rotation in all three Euler angles of polyatomic molecules (Larsen *et al.*, 2000). Having explored the role played by the laser frequency, the pulse duration and the rotational temperature in the previous subsection, we confine attention here to the case of nonresonant adiabatic alignment at zero temperature and focus on the role played by the field polarization.

At nonresonance frequencies, well below electronic transition energies, the field-matter interaction can be cast in the form of an induced Hamiltonian,

$$H_{\text{ind}} = -\frac{1}{4} \sum_{\rho,\rho'} \varepsilon_\rho \alpha_{\rho\rho'} \varepsilon_{\rho'}, \qquad (2)$$

where $\rho,\rho' = x,y,z$ denote the space-fixed coordinates and α is the molecular polarizability tensor. In Eq. (2) we have expressed the laser field as $\epsilon(t) = \varepsilon(t)\cos(\omega t)$, where $\varepsilon(t)$ is a smooth envelope and ω is the laser frequency. The derivation of H_{ind} from the electric dipole interaction, $\vec{\mu} \cdot \vec{\epsilon}$, relies on the assumption that the frequency is far-detuned from vibronic transitions (Pershan, van der Ziel, and Malmstrom, 1966; Seideman, 1999b). One expresses the complete wave packet as a superposition of rovibronic states of the field-free Hamiltonian and inserts the expansion in the time-dependent Schrödinger equation, to obtain a set of coupled equations for the expansion coefficients. Adia-

batic elimination of the vibronic states in which real population does not reside leads to the interaction (2), where time-dependence arises only from the pulse envelope (Pershan, van der Ziel, and Malmstrom, 1966; Seideman, 1999b).

The space-fixed components of the polarizability tensor, $\alpha_{\rho\rho'}$ in Eq. (2), are related to its body-fixed components $\alpha_{kk'}$ by

$$\alpha_{\rho\rho'} = \sum_{kk'=X,Y,Z} \langle \rho|k \rangle \alpha_{kk'} \langle k'|\rho' \rangle, \qquad (3)$$

where $\{X,Y,Z\}$ are the body-fixed Cartesian axes and $\langle k|\rho \rangle$ are transformation elements (often referred to as direction cosines). Table 1 of Seideman (1996) provides expressions for the $\langle k|\rho \rangle$ in terms of the Euler angles of rotation, $\{\phi,\theta,\chi\}$, relating the body- and space-fixed frames.[3] Substitution of these expressions in Eq. (2) provides useful insight into the forces that act to align the molecule with different choices of the polarization, which we proceed to discuss.

In the case of a linear or a symmetric top molecule ($\alpha_{ZZ} = \alpha_\parallel$, $\alpha_{XX} = \alpha_{YY} = \alpha_\perp$) interacting with a linearly polarized field ($\varepsilon = \varepsilon_z$), the interaction term depends on only one angle, the polar Euler angle θ between the field and molecular axis. Equation (2) is then readily seen to reduce to

$$H_{\text{ind}} = -\frac{1}{4}\varepsilon^2(\alpha_\parallel - \alpha_\perp)\cos^2\theta \qquad (4)$$

(apart from an angle-independent term that merely shifts all eigenvalues). The term in $\cos^2\theta$ is responsible for the nonconservation of the total angular momentum, see Fig. 1(b). The symmetry of H_{ind} with respect to $\theta \to \pi - \theta$ results in conservation of parity; only J levels of the same parity interfere in the wave packet of Fig. 1. The independence of H_{ind} of the azimuthal Euler angles, ϕ and χ, results in conservation of M and K. Put alternatively (but equivalently), Eq. (4) provides an effective well for the angular motion that converts the free rotation into small amplitude librations. It does not, however, orient the molecule and does not hinder the free rotation about the field axis or, in the nonlinear case, the free rotation about the molecular symmetry axis.

Similarly, a circularly polarized field ($\varepsilon_z = 0$, $|\varepsilon_x| = |\varepsilon_y| \neq 0$) interacting with a linear or a symmetric top molecule ($\alpha_{ZZ} = \alpha_\parallel$, $\alpha_{XX} = \alpha_{YY} = \alpha_\perp$) gives rise to a ϕ- and χ-independent interaction of the form

$$H_{\text{ind}} = \frac{1}{8}\varepsilon|^2(\alpha_\parallel - \alpha_\perp)\cos^2\theta \qquad (5)$$

(up to an overall shift). Consequently the molecular symmetry axis aligns parallel (perpendicular) to the po-

---

[3]Here θ is the polar Euler angle between the space- and body-fixed z axes, ϕ is the azimuthal angle of rotation about the space-fixed z axis, and χ is the azimuthal angle of rotation about the body-fixed z axis.
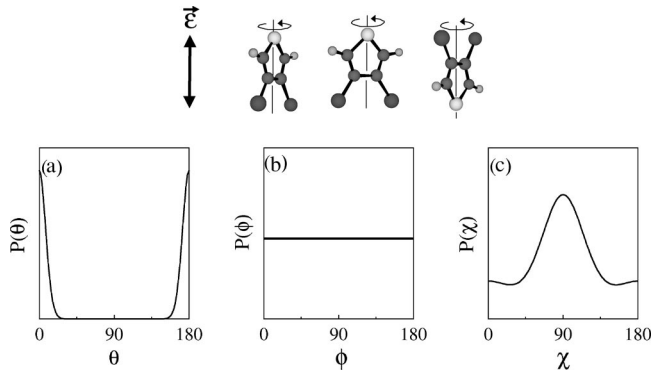
FIG. 3. Alignment of 3,4-dibromothiophene (DBT) in a linearly polarized field. The pulse duration is 3.5 ns and the intensity is 5.4×10^{11} W cm^{-2}. Panels (a), (b), and (c) show, respectively, the probability density at the peak of the field vs θ, ϕ, and χ. The ordinate labels are omitted for clarity but we remark that the scale is linear and that the ordinate in panel (a) spans a factor of 40 larger range than that in panel (c). The inset shows a ball-and-stick model of DBT subject to a linearly polarized field.

larization plane for $\alpha_\parallel > \alpha_\perp (\alpha_\parallel < \alpha_\perp)$ but its motion in the two azimuthal Euler angles remains free.

In the case of an asymmetric top molecule, the interaction term becomes χ dependent;

$$H_{\text{ind}} = -\frac{1}{4}[\varepsilon^2 \sin^2 \theta(\alpha_{XX}\cos^2 \chi + \alpha_{YY} \sin^2 \chi)$$
$$+ \cos^2 \theta \alpha_{ZZ}], \qquad (6)$$

assuming the field to be linearly polarized, and hence the rotation about the body-fixed z axis is not rigorously free, although not well defined, see the inset of Fig. 3. The slight anisotropy of the χ motion corresponds to the nonconservation of K in asymmetric top molecules. The rotation about the laser polarization vector remains unhindered.

In the presence of an elliptically polarized field the Hamiltonian depends on ϕ, and M is no longer conserved. In the general case of an asymmetric top, H_{ind} is a function of all three Euler angles, giving rise to the coherent excitation of a wave packet that is broad in J, M, and K and correspondingly well defined in θ, ϕ, and χ.

These general results are illustrated for the specific case of 3,4-dibromothiophene (DBT) in the main frames of Figs. 3, 4, and 5 for linear, circular, and elliptical polarizations, respectively. In each of the three figures, panels (a), (b), and (c) give the probability density at the peak of the pulse vs θ, ϕ, and χ, respectively; $P(\theta) = \int d\phi d\chi |\Psi(\theta, \phi, \chi)|^2$, etc. Panels (d), (e), and (f) of Fig. 5, corresponding to elliptical polarization of the field, illustrate the dynamics in the conjugate space through the expectation values of (d) J, (e) M, and (f) K vs time during the adiabatic turn-on of the pulse. The intensity, ellipticity, and pulse duration are chosen to correspond to the experiments described in Sec. III.C. In the linear polarization case the wave packet is confined to $\theta \sim 0, \pi$ while the ϕ dependence is isotropic, corre-
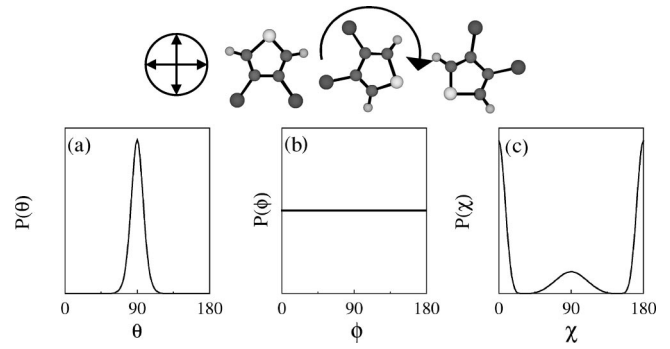
sponding to sharply defined M, and the χ motion is slightly hindered. Similarly, a circularly polarized field leaves ϕ undefined, corresponding to free rotation of the molecular plane in the polarization plane. An elliptically polarized field populates a broad superposition of J, M, and K, states that is sharply defined in θ, ϕ, and χ.

Our choice of DBT as a model to explore the opportunities offered by the laser polarization is due to the suitability of this system to our experimental detection technique, see Sec. III.C. We remark that the concept is general.

III. EXPERIMENTAL OBSERVATION OF ALIGNMENT

A. One-dimensional adiabatic alignment

In Sec. II we showed that the rotational eigenstates and eigenenergies of a molecule are significantly changed when it is exposed to a strong laser field. It should therefore be possible to observe alignment by performing rotational spectroscopy—an approach taken
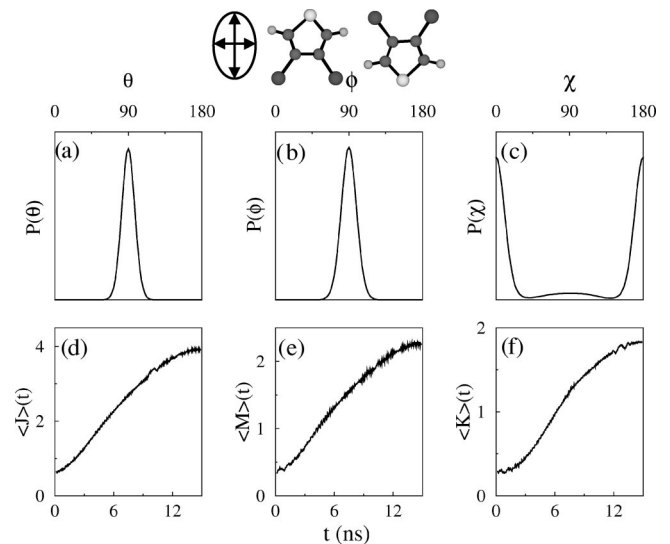

FIG. 4. As in Fig. 3 for a circularly polarized field.

FIG. 5. As in Fig. 3 for an elliptically polarized field. The intensity is 5.4×10^{11} W cm^{-2} along the major axis and 1.1×10^{11} W cm^{-2} along the minor axis. Panels (d), (e), and (f) show, respectively, the expectation value of J, M, and K in the wave packet vs time during the adiabatic turn-on.
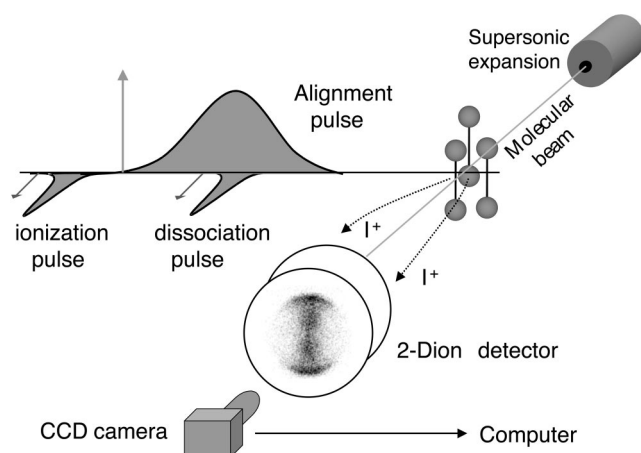
FIG. 6. The experimental setup used for observation of adiabatic alignment, showing the molecular beam, the different laser pulses, and the two-dimensional ion imaging system. The extraction field deflecting the ions towards the detector is not displayed. The polarization direction of each laser field is indicated by an arrow.

FIG. 7. Ion images of I^+ recorded for different YAG pulse intensities and for I_2 seeded in helium or in argon. The polarization and the intensity of the YAG pulse is indicated at each image. The dissociation and the ionization pulses are linearly polarized perpendicular to the image plane [i.e., along the molecular beam (see Fig. 6)].

by Felker and co-workers (Kim and Felker, 1996). Using stimulated Raman transitions between rotational/pendular states of naphthalene trimer molecules, with one of the Raman laser pulses simultaneously providing the strong alignment field, they observed a clear change of the spectrum as the field was increased from zero to 4×10^{10} W cm^{-2}. This experiment provided the first unambiguous observation of laser-induced alignment and enabled a determination of the degree of alignment, $\langle \cos^2 \theta \rangle = 0.58$. The group has subsequently used the Raman technique to detect alignment of several other molecules (Kim and Felker, 1997). An analysis of these results is given in Kim and Felker (1998).

An alternative method of quantifying intense laser alignment is by photodissociating them in the presence of the alignment field and recording the direction of the photofragments. The experimental setup for observation of alignment, employing this technique, is shown in Fig. 6 (Larsen *et al.*, 1998; Sakai, Safvan, *et al.*, 1998; Larsen, Sakai, *et al.*, 1999). A small fraction, typically 1% or less, of a molecular gas is mixed with 1–4 bars of helium or 1 bar of argon and expanded through a nozzle into a vacuum chamber. The supersonic, rotationally cold molecular beam is skimmed and crossed at 90° with three pulsed laser beams. One of the laser beams consists of 3.5-ns-long, almost transform limited pulses at 1064 nm originating from a Nd:YAG (yttrium aluminum garnet) laser. These pulses are used to adiabatically align the molecules. The maximum intensity used is 1.4 $\times 10^{12}$ W cm^{-2}. Since the molecules are only aligned when the YAG field is on, measurement of the molecular alignment must be performed in the presence of the field. For the first alignment experiment, performed on iodine molecules (Sakai, Safvan, *et al.*, 1998; Larsen, Sakai, *et al.*, 1999), this was done by dissociating the I_2 molecules with a femtosecond laser pulse at 688 nm synchronized to the peak intensity of the YAG pulse. The
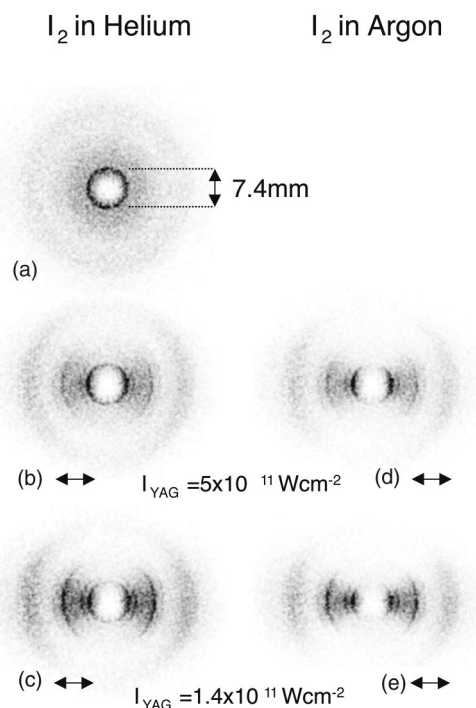
intensity of the 688-nm pulse, 3×10^{12} W cm^{-2}, is low enough to avoid saturation of the dissociation. The photodissociation of I_2 is direct and hence the photofragments fly out in the direction of the molecular axis. Therefore, the photofragment angular distribution provides a direct measure of the alignment of the molecule. To measure the angular distribution, the photofragments are ionized and accelerated by a weak static electric field towards a two-dimensional ion detector (Eppink and Parker, 1997). The ionization is done by a second, intense (7×10^{13} W cm^{-2}), 100-fs-long laser pulse arriving 200 ps after the dissociation pulse. The two-dimensional ion images are recorded by a charge-coupled device camera and stored on a computer. The images make it possible to determine both the angular and the energy distribution of the photofragments.

Examples of the two-dimensional I^+ ion images for the first alignment experiment, performed on I_2 molecules, are shown in Fig. 7. In Fig. 7(a) there is no YAG laser pulse present and the angular distribution of the photofragments, corresponding to the dark prominent ring with diameter 7.4 mm, is isotropic. When the strong YAG field is applied, polarized horizontal in the figure, the circular symmetry of the ion image is broken [Figs. 7(b)–7(e)], and the photofragments emerge in a narrow distribution centered along the YAG polarization. Keeping the intensity of the YAG pulse fixed but seeding the I_2 molecules in argon rather than in helium leads to a stronger angular confinement [compare Fig. 7(b) with 7(d), or 7(c) with 7(e)]. It is well known that using
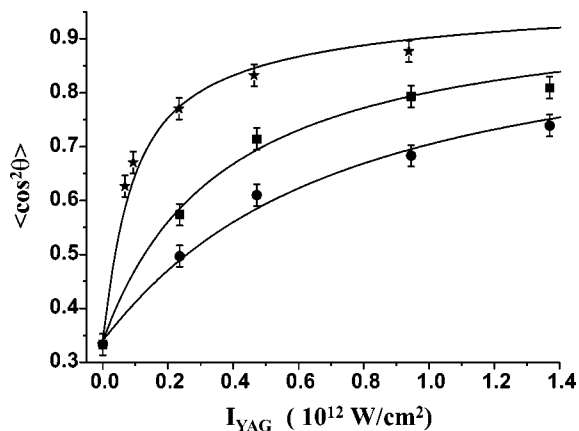
FIG. 8. The observed value of $\langle \cos^2 \theta \rangle$ for different I_{YAG} and for I_2 seeded in 1 bar He (circles), 1 bar Ar (squares), and 4 bar He (stars). The full curves are calculated values of $\langle \cos^2 \theta \rangle$.

FIG. 9. Ion images of I^+ recorded when iodobenzene is irradiated by a circularly polarized, 100-fs, 8×10^{13}-W/cm^2, 800-nm pulse. (a) No alignment field. (b) In the presence of a linearly polarized (vertical) alignment field with intensity 1.2×10^{12} W/cm^2. The spatial orientation of the molecules is illustrated below the two images.

argon instead of helium as a carrier gas for iodine leads to lower rotational temperature. We therefore interpret the stronger angular confinement observed with argon than with helium as a result of better alignment due to lower initial rotational temperature. Keeping the carrier gas fixed but increasing the YAG intensity also leads to better angular confinement with both He and Ar carrier gases [compare Fig. 7(b) with 7(c), or 7(d) with 7(e)]—in accordance with the interpretation of alignment.

The results of the 2D ion images are summarized in Fig. 8. Here, the degree of alignment, expressed as $\langle \cos^2 \theta \rangle$ (θ being the angle between the YAG polarization axis and the molecular axis), is plotted as a function of the YAG intensity and for a carrier gas of 1 bar He (circles), 1 bar Ar (squares), and 4 bar He (stars), respectively. (The ion images obtained with 4 bar He are not shown in Fig. 7.) The full curves are the calculated results obtained by a numerical solution of the time-independent Schrödinger equation assuming a rotational temperature of 7 K for 1 bar He, 3.5 K for 1 bar Ar, and 1 K for 4 bar He. For the highest degree of alignment observed, corresponding to $\langle \cos^2 \theta \rangle = 0.88$, about 60% of all the molecules have their axis located within a cone of 30° full width at half maximum. For a comparison, this number is only 3.4% when the molecules are randomly oriented.

As mentioned in Sec. II, alignment by a strong laser field is applicable to all molecules possessing an anisotropic polarizability. We carried out experiments on a number of different molecules, in addition to I_2, and observed alignment of the linear molecules ICl, CS_2, the symmetric top molecule CH_3I (Sugita *et al.*, 2000), and the asymmetric top molecules C_6H_5I, C_6H_5Br, o-$C_6H_4Br_2$, p-$C_6H_4Br_2$, and 3,4 $C_4H_2SBr_2$. Using Raman spectroscopy, Felker and co-workers showed that naphthalene trimers and Ar-benzene complexes can also be aligned (Kim and Felker, 1997). As an example, in Fig. 9, we show some of the ion images that identify alignment of iodobenzene (Larsen, Sakai, *et al.*, 1999). The measurement is performed by Coulomb exploding the molecules with an intense, circularly polarized femtosecond laser pulse (discussed in more detailed in the
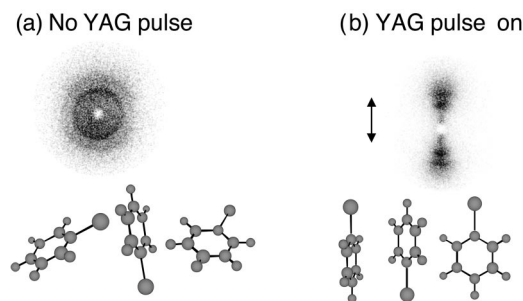
next section), synchronized to the peak intensity of the alignment (YAG) pulse, and recording the direction of I^+ fragments by the 2D ion detector. In Fig. 9(a) there is no alignment pulse present and the angular distribution of the I^+ ions is almost uniform. By contrast, when the alignment pulse is on, Fig. 9(b), the ion angular distribution is strongly peaked around the YAG polarization. Similar to the I_2 experiment the degree of alignment increases when the intensity of the YAG pulse is increased and when the rotational temperature of iodobenzene is decreased (Larsen, Sakai, *et al.*, 1999).

In general, for a given molecule, the degree of (adiabatic) alignment can be optimized by increasing the intensity of the alignment field or by lowering the rotational temperature of the molecule. The maximum intensity that can be applied to the molecule is limited by tunnel (or multiphoton) ionization or by multiphoton dissociation. For an I_2 molecule ionization by a few ns long YAG pulse will become significant at around 10^{13} W/cm^2 (Dietrich and Corkum, 1992). Optimizing the supersonic expansion molecules can be rotationally cooled down to 1–2 K or a bit lower (Even *et al.*, 2000). For such cold molecules it should be possible to achieve a degree of alignment of ~0.90 by exposing the molecules to the strongest alignment field that still leaves them intact in their ground state. Recently, Legare and Bandrauk (2001) suggested that the degree of alignment can be further improved by photodissociating those molecules that are the least aligned.

B. One-dimensional nonadiabatic alignment

As illustrated in Sec. II.A.2, molecules can be aligned also with laser pulses that are shorter than the rotational period. A first experimental demonstration of such nonadiabatic alignment was recently reported by Rosca-Pruna and Vrakking (2001, 2002a). These authors employed a 4.2-ps, 10^{13}-W/cm^2, 800-nm pump pulse to align I_2 molecules. To detect and characterize the alignment, they irradiated the molecules with an intense (5×10^{14} W/cm^2) 100-fs, 800-nm probe pulse. The I^+ and I^{2+} ions produced through multielectron dissociative
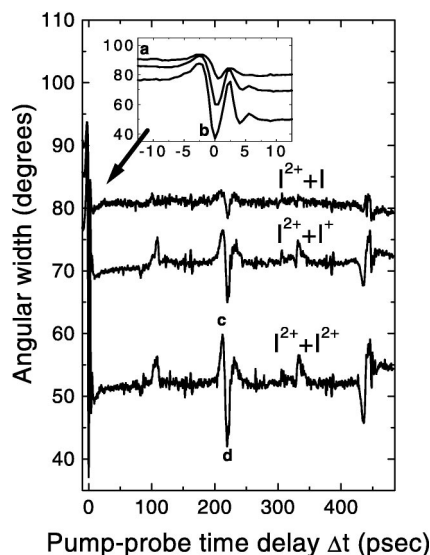
FIG. 10. Pump-probe delay scan showing the I^{2+}-I, I^{2+}-I^+, I^{2+}-I^+ channels. The measurements show alignment of the molecule during the pump pulse (see inset), residual alignment at the end of the pulse, and the occurrence of rotational revivals. [Reprinted with permission from Phys. Rev. Lett. **87**, 153902 (2001). ©2001 The American Physical Society.]

ionization (MEDI) were recorded with a two-dimensional ion imaging system similar to that described in Sec. III.A. By setting the polarization of the probe laser perpendicular to the detector plane the authors ensured that in the absence of the alignment pulse the images are circularly symmetrical. Any deviations from circular symmetry detected in the presence of the pump pulse could thus be ascribed to laser induced alignment.[4] The time evolution of the alignment was probed by repeating the experiment for a series of time delays between the pump and probe pulses. Figure 10 shows the effective angular width extracted from the two dimensional ion images. All MEDI channels (I^{2+}-I, I^{2+}-I^+, I^{2+}-I^{2+}) are seen to exhibit the same qualitative behavior. At short times the angular width decreases to a minimum, showing that the molecules reach a maximum degree of alignment around the peak of the pump pulse. At later times the wave packet dephases and the angular width remains constant near (but yet below) the isotropic value. This mild alignment corresponds to the $\langle \cos^2 \theta \rangle \approx 0.5$ plateau regimes of Fig. 2(c) and its origin is explained in Sec. II.A.2. At a delay time of ~220 ps between the pump and probe pulses the angular width exhibits a sharp structure, corresponding to the half revival time, see Fig. 2(c). Also seen clearly in Fig. 10 is the full revival of the I_2 wave packet at $\Delta t \sim 440$ ps, where the aligned wave packet produced at $\Delta t = 0$ is precisely reconstructed.

Rosca-Pruna and Vrakking confirmed their observations of nonadiabatic alignment by varying the intensity

---

[4]This requires that the pump-laser-only does not produce any I^+ or I^{2+} ions.

of the pump pulse and the rotational temperature of the molecules. A quantitative comparison between the observations and numerical calculations is given in Rosca-Pruna and Vrakking (2002a, 2002b).

C. Three-dimensional adiabatic alignment

In the previous section we illustrated that a strong linearly polarized laser pulse of sufficiently long duration can align the largest polarizability axis of a molecule along a given direction fixed in space. For iodobenzene this is the symmetry axis. The two other principal axes of the molecule are virtually unaffected by the strong field. In the case of iodobenzene this means that the molecular plane is still free to rotate about the polarization axis, as illustrated in the lower part of Fig. 9(b). In Sec. II.B we described how it is possible to achieve three-dimensional alignment of a polyatomic molecule by using an elliptically polarized laser field. In this section we discuss the experimental observation of three-dimensional alignment (Larsen *et al.*, 2000).

Specifically, we use 3.5-ns-long YAG laser pulses at 1064 nm, made elliptically polarized by a quarter wave plate, to align 3,4 dibromothiophene (3,4 DBT) molecules. The major axis of the polarization can be positioned either perpendicular or parallel to the detector plane. To probe the molecular alignment we Coulomb explode the DBT molecules with an intense (5×10^{14} W cm^{-2}) 20-fs laser pulse, synchronized to the peak intensity of the YAG pulse. The intense probe pulse removes several electrons so rapidly from the molecule that the molecular skeleton is unchanged immediately after the pulse. In the subsequent Coulomb explosion of the molecules the S^+ ions are ejected along the symmetry axis and the Br^+ ions are ejected in the plane of the molecule. Recording of the direction of both the S^+ and the Br^+ ions therefore enables us to determine the degree of 3D alignment.

In Fig. 11 we show the 2D ion images of S^+ and Br^+ for different ellipticities, i.e., different ratios between the intensity along the major and minor axis, and for the major axis perpendicular (upper images) and parallel to the detector plane (lower images). In the absence of the YAG pulse [Fig. 11 (A1)–(A4)] both the S^+ and Br^+ ion images are circularly symmetric, showing that the DBT molecules are initially randomly oriented. When the YAG pulse is linearly polarized, the S^+ ions become localized about the polarization axis as seen on Fig. 11 (B4), where the YAG polarization is parallel to the detector plane. This observation is similar to the localization of the I^+ ions when iodobenzene is exposed to a strong linearly polarized YAG pulse [Fig. 9(b)] and proves that the symmetry axis of DBT is aligned along the YAG polarization. At the same time, the Br^+ image, recorded with the polarization (major) axis perpendicular to the detector plane [Fig. 11 (B1)], is circularly symmetric. This shows that the there is no alignment of the molecular plane. However, when an elliptical field is used, the circular symmetry of the Br^+ image is broken and the Br^+ ions are localized along the direction of the
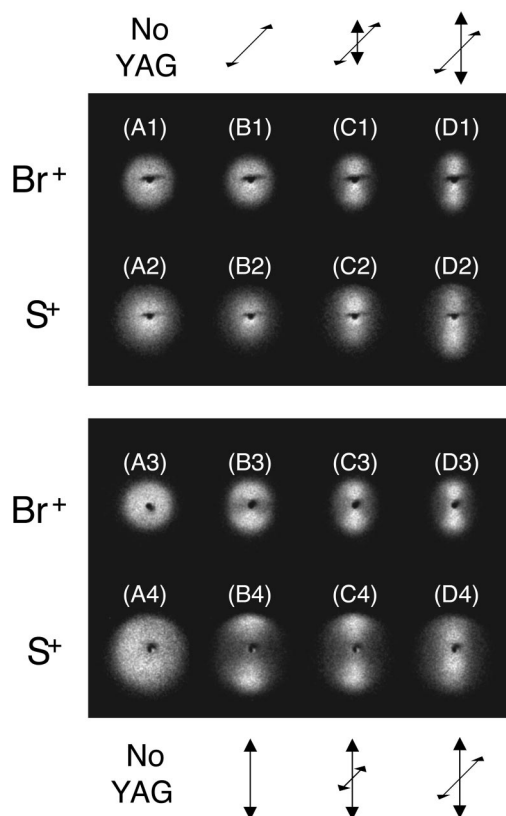
FIG. 11. Ion images of Br^+ and S^+ recorded for different ellipticities of the alignment field. (A) No alignment field. (B) Linearly polarized alignment field with $I_{YAG}=5.4 \times 10^{11}$ W/cm^2. (C) Elliptically polarized alignment field with $I_{YAG,major}=5.4\times10^{11}$ W/cm^2 and $I_{YAG,minor}=1.1 \times10^{11}$ W/cm^2. (D) Circularly polarized alignment field with $I_{YAG,major}=I_{YAG,minor}=5.4\times10^{11}$ W/cm^2. The major axis is either perpendicular (upper images) or parallel (lower images) to the detector plane (indicated by arrows above or below the images).

minor field [Fig. 11 (C1)]. The localization becomes stronger as the relative strength of the minor field is increased (not shown in Fig. 11), demonstrating that the molecular plane is aligned with the polarization plane. Returning to the S^+ images recorded for the major axis parallel to the detector plane, it is seen that the localization of S^+ ions along the major axis persists as the pulse is made elliptically polarized [compare Fig. 11 (B4) and (C4)]. The simultaneous observations of the S^+ and the Br^+ ion images demonstrate that an elliptically polarized field can three dimensionally align molecules. Finally, when a circularly polarized pulse is used, the molecular plane is strongly aligned [Fig. 11 (D1)]. However, the S^+ image has changed from two localized regions [Fig. 11 (C4)] to a narrow band [Fig. 11 (D4)] similar to the Br^+ image. This shows that the S^+ ions are ejected in the polarization plane rather than along a fixed axis. We conclude that the DBT molecule is aligned to the polarization plane but free to rotate within that plane.

The three-dimensional alignment is generally applicable to molecules that possesses different polarizabilities along three molecular axes. The ellipticity necessary to optimize the degree of alignment depends on the specific polarizability tensor. In the case of a planar molecule, like iodobenzene, the optimum alignment of the molecular plane is obtained by using a circularly polarized field. When an elliptically polarized field is applied to produce alignment of the symmetry axis, the plane of the molecule will be less strongly confined. Thus, the choice of the ellipticity depends upon the actual requirements of the particular application in which the three-dimensionally aligned molecules are used.

IV. APPLICATIONS OF ALIGNMENT

A variety of new and exciting applications of laser-aligned molecules are currently emerging. In one study, Velotta and co-workers (2001) use 300-ps laser pulses to align high-density molecular vapors and exploit the aligned medium for high-order harmonic generation. Consistent with expectation Lappas and Marangos, (2000), Vellotta *et al.* (2001) demonstrate enhancement of the harmonic intensity as compared to the random orientation case. Another novel application is proposed in the works of Kalosha *et al.* (2002) and Bartels *et al.* (2002), where the possibility of using laser-aligned molecules to generate and shape ultrashort pulses is demonstrated theoretically (Kalosha *et al.*, 2002) and experimentally (Bartels *et al.*, 2002). Here a short pulse (Bartels *et al.*, 2002) or a long turn-on, rapid turn-off pulse of the form of Eq. (1) is used to generate a medium with a time-modulated refractive index (Kalosha *et al.*, 2002). It is shown that a delayed probe pulse sent into the medium can be engineered so as to emerge compressed. Bhardwaj *et al.* (2001) discuss the potential role of laser alignment in studies of strong field electron recollision events, where electrons released into an oscillating laser field through tunnel ionization are driven by the field to rescatter from the parent ion core (Hoshina *et al.*, 2002). The possibility of using 3D alignment (Secs. II.B and III.C) to produce a time-periodic molecular switch, proposed in Seideman (2001a), is under theoretical investigation. In this section we expand on two applications; the first (Sec. IV.A) exemplifying the use of intense laser alignment as a control tool, and the second (Sec. IV.B) exemplifying its use as an analytical tool.

A. Control of photoabsorption/photodissociation

In general, absorption of polarized light by molecules depends on the alignment of the molecule with respect to the polarization direction. Therefore, by controlling the angle between the polarization vectors of an exciting laser field and an aligning laser field one can preferentially populate through photoexcitation an electronic state of a given symmetry, while suppressing the population of states of different symmetries. In this section we illustrate this state selectivity in electronic photoexcitation through the example of iodine, and show how
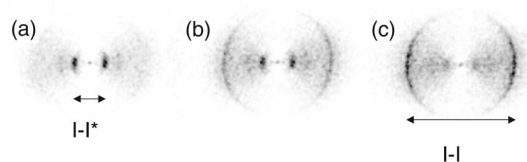
FIG. 12. Ion images of I^+ resulting from photodissociation of aligned I_2 molecules. In all images the alignment field polarization is horizontal. The angle between the polarization of the alignment and the dissociation fields is (a) 0°, (b) 45°, (c) 90°.

it allows control of the branching ratio of two photodissociation channels (Larsen, Wendt-Larsen, and Stapelfeldt, 1999).

When I_2 molecules are irradiated by blue light at around 485 nm, they are excited to either the B $^3\Pi_0$ state, through a parallel transition, or to the $^1\Pi_1$ state, through a perpendicular transition.[5] The extinction coefficients for the two excitation pathways are approximately equal at 485 nm. Following excitation, the molecules in the B $^3\Pi_0$ state dissociate into $I+I^*$ (I^* denotes the upper fine-structure state of the iodine atom), and the molecules in the $^1\Pi_1$ state dissociate into $I+I$. Using aligned I_2 molecules the branching ratio of the two dissociation channels is controlled simply by polarizing the dissociation laser either parallel to the alignment axis ($I+I^*$) or perpendicular to the alignment axis ($I+I$).[6]

The experimental technique is similar to that described in Sec. III.A. A linearly polarized YAG laser pulse aligns the I_2 molecules and the dissociation pulse (150 fs long, centered at 485 nm) is synchronized to the peak intensity of the YAG pulse. The photofragments are detected by ionizing them with an intense, 800-nm, 100-fs-long pulse, delayed 200 ps with respect to the dissociation pulse.

In Fig. 12 we show three ion images recorded for the dissociation pulse polarized at an angle of (a) 0°, (b) 45°, and (c) 90° with respect to the YAG polarization. The two dissociation channels are identified by the radial position in the ion image. The $I+I$ channel produces photofragments with high translational energy, detected as a pair of rings with large radii, and the $I+I^*$ produces photofragments with low translational energy, detected as a pair of rings with small radii. The images show that, for the dissociation pulse polarized parallel to the YAG polarization, virtually all I_2 molecules dissociate through the $I+I^*$ channel. By contrast, in the perpendicular geometry, the $I+I^*$ channel essentially disappears and instead all molecules dissociate through the $I+I$ channel. When the angle between the dissociation pulse and the YAG polarization is 45° there is an approximately equal contribution from the two dissociation channels.

In polyatomic molecules, selectivity in photoexcitation will not always provide control of electronic branching ratios. Depending on the details of the system, a certain selectivity of the dissociation channels or control of the mechanism of photodissociation can be achieved. As an example we consider the photodissociation of iodobenzene by near uv irradiation.

When iodobenzene is irradiated by uv light at 240–280 nm, the C-I bond breaks. This occurs either directly, via a $n\rightarrow\sigma^*$ transition, or by a vibronic excitation of the benzene ring ($\pi\rightarrow\pi^*$) and subsequent coupling between vibrational and electronic motion. The $n\rightarrow\sigma^*$ channel is dominated by a parallel transition (transition dipole moment along the C-I bond) with a minor contribution from a perpendicular transition, whereas the $\pi\rightarrow\pi^*$ channel has a transition dipole moment in the plane of the molecule. We have aligned iodobenzene molecules with a linearly polarized YAG laser and shown that both the $n\rightarrow\sigma^*$ channel and the $\pi\rightarrow\pi^*$ channel are enhanced when the dissociation laser is polarized parallel to the YAG polarization and suppressed when it is polarized perpendicular to the YAG polarization (Poulsen, Skovsen, and Stapelfeldt, 2002). The enhancement and the suppression are strongest for the $n\rightarrow\sigma^*$ channel because of its dominance by a parallel transition. The control of the photodissociation channels will be more complete upon using three-dimensionally aligned molecules. By polarizing the dissociation laser in the molecular plane perpendicular to the symmetry axis the $n\rightarrow\sigma^*$ channel will be suppressed down to the contribution from the minor perpendicular component, whereas the $\pi\rightarrow\pi^*$ channel will be maximized. By contrast, if the dissociation laser is polarized perpendicular to the molecular plane, the $\pi\rightarrow\pi^*$ channel will be suppressed but the $n\rightarrow\sigma^*$ channel will remain intact due to its perpendicular component. This experiment is yet to be performed.

B. Probe of nonradiative transitions

The problem of radiationless transitions (internal conversions and intersystem crossings) has been the topic of several decades of intensive research, this being one of the most general phenomena in excited state dynamics.[7] In recent years much effort has been devoted to the application of time-domain methods to probe the dynamics of nonradiative transitions (Seel and Domcke, 1991; Kim, Schick, and Weber, 1995; Radloff *et al.*, 1997; Blanchet *et al.*, 1999). Here, one is predominantly interested in internal conversions, which are often ultrafast and difficult to study in the energy domain. Essential to the application of pump-probe techniques to study nonradiative transitions is an observable that can be measured as a function of the delay between the pump and probe pulses and that undergoes a substantial change upon transition.

———

[5]A transition of a linear molecule is called parallel (perpendicular) if its transition dipole moment is parallel (perpendicular) to the internuclear axis—see Zare (1988).

[6]Related results have been obtained on molecular chlorine; see Sugita *et al.* (2001).

———

[7]For an early review of the problem of nonradiative transitions, see Jortner, Rice, and Hochrasser (1969).
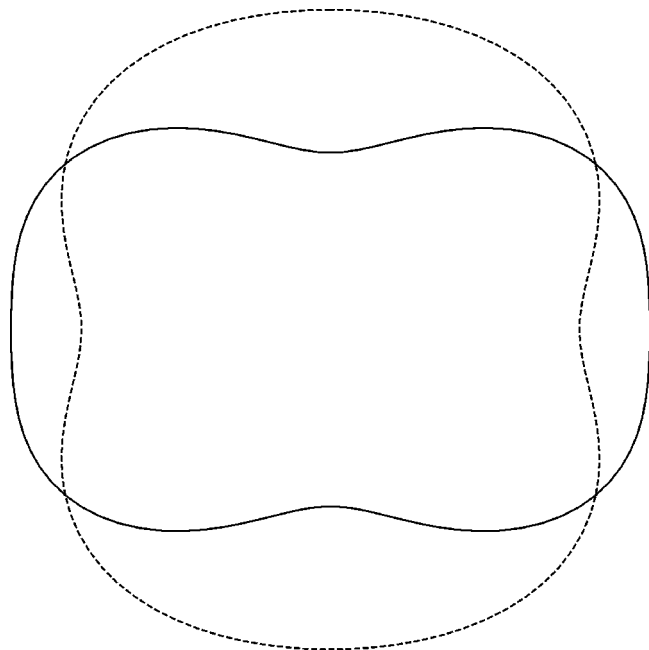
FIG. 13. The application of alignment in time-resolved studies of nonradiative transitions. Two snapshots of a time-evolving photoelectron angular distribution probing the internal conversion between the optically bright (S_2) and dark (S_1) states of model pyrazine: At $\Delta t = 60$ fs, when the wave packet resides mostly in the dark state (dashed curve), and after a time τ_{IC} ~30 fs, when the bright state population is maximized (solid curve). The space-fixed z axis is horizontal. The details of the model are described in Suzuki, Stener, and Seideman (2002).

Seideman (2000, 2001b) proposed the possibility of using time-resolved photoelectron angular distributions (PAD's)[8] as a probe of nonradiative transitions and illustrated this opportunity through a numerical example. The PAD was found to undergo a qualitative change upon internal conversion between the optically bright (S_2) and dark (S_1) states of a long-chain linear polyene (Seideman, 2000, 2001b). A first experimental realization of the theory has been recently reported (Hayden, 2002). Specifically, a substantial change of the measured PAD was found to accompany internal conversion between the bright and dark states of triethylenediamine (Hayden, 2002). Figure 13 shows two snapshots of the time evolution of PAD's from a model calculation of the internal conversion of pyrazine (Suzuki, Stener, and Seideman, 2002). The dashed curve is taken at a pump-probe delay $\Delta t = 60$ fs, when the population of the dark state is maximized, reaching ~70%. The solid curve, taken at a time τ_{IC} ~30 fs later (where τ_{IC} is the internal conversion time), $\Delta t = 90$ fs, when the bright state population is maximized, reaching ~50%.

The origin of the sensitivity of time-resolved PAD's to electronic coupling is traced in Seideman (2000, 2001b) to the mild alignment that is induced by the pump field

---

[8]For a review of the concept, theory, and applications of time-resolved photoelectron angular distributions, see Seideman (2002).

and is present in all pump-probe experiments. If the two coupled states differ in electronic symmetry, their ionization to a common state of the ion produces electronic waves of different symmetry. This follows from the requirement that the product of irreducible representations of the neutral electronic state, the dipole operator, the free electronic state, and the ion-core electronic state would contain the totally symmetric representation of the relevant point group. Consequently, the electronic distribution with respect to the molecular axes undergoes a change as the system transforms between the bright and dark states. Alignment of the molecule is necessary in order for the change of electronic symmetry in the *molecular* frame to translate into a change of the angular distribution in the *laboratory* frame. In the cases studied in Seideman (2000, 2001b) and Hayden (2002) the mild alignment induced by the weak pump pulse suffices to that end. Nonetheless, sharper alignment enhances the sensitivity of the PAD to the symmetry change and may be necessary for an effect to be observed in other cases. This can be achieved either by using a moderately intense pump pulse to affect near-resonance alignment or by prealigning the molecules prior to the femtochemistry experiment with a short nonresonance pulse. In both cases one capitalizes on the field-free alignment that is available after the turn-off when the pulse is short with respect to rotational periods (see Sec. II.A.2). Strong field effects in the observation of internal conversions using time-resolved PAD's are explored in Suzuki, Stener, and Seideman (2002).

As discussed in Sec. II.B, a linearly polarized (near or far-off-resonance) field leaves the molecule rotating freely about one or two axes. Depending on the molecular symmetry and on the type of the pump-induced transition, this rotation may be expected, and was numerically found, to severely degrade the sensitivity of the PAD to the electronic coupling. One may thus expect that the ability of the 1D alignment induced by the (weak or strong) pump to translate the symmetry change into a laboratory frame observable would depend heavily on system properties. The use of an elliptically polarized prealigning pulse to affect 3D alignment is expected to provide a more general tool, capable of enhancing the sensitivity of time-resolved PAD's to electronic coupling when it is naturally available, or building-in such sensitivity in other cases. This opportunity remains to be investigated numerically.

V. CONCLUSION

Intense laser fields can align molecules along a given space-fixed axis, force them to a plane, or eliminate their rotations altogether, by choice of the polarization to linear, circular, or elliptical, respectively. From the theoretical viewpoint, the basic physics of intense laser alignment is now understood in both static and dynamic regimes. Several fundamental questions are likely to form the topic of further numerical research in this area. These include the controllability of 3D alignment (Larsen *et al.*, 2000) in particular in the dynamical re-

gime, the problem of rovibrational wave packets with their peculiar revival structure (Althorpe and Seideman, 2000), and the problem of intense field orientation (Friedrich and Herschbach, 1999; Henriksen, 1999; Averbukh and Arvieu, 2001; Dion, Keller, and Atabek, 2001; Machholm and Henriksen, 2001; Dion *et al.*, 2002; Guerin *et al.*, 2002). We believe, however, that the main topic of future theoretical and numerical work in this field will be novel applications of aligned molecules.

From the experimental viewpoint, adiabatic alignment is well documented, but more work should be carried out on three-dimensional alignment, in particular, on quantifying the degree of alignment and the meaning of an optimum ellipticity. A key issue is dynamical alignment, a field that recently saw the first demonstration of linear alignment (Rosca-Pruna and Vrakking, 2001). First experimental demonstrations of orientation through a combination of a laser field and a static electric field (Friedrich and Herschbach, 1999) were recently reported (Baumfalk, Nahler, and Buck, 2001; Sakai *et al.*, 2003). Experimental tests of other intense-laser-based schemes (Henriksen, 1999; Averbukh and Arvieu, 2001; Dion, Keller, and Atabek, 2001; Machholm and Henriksen, 2001; Dion *et al.*, 2002; Guerin *et al.*, 2002) may be expected to form another topic of future experimental research. Efficient alignment and orientation in the liquid phase remains an interesting problem, theoretically and experimentally.

In closing, we note that alignment is only one consequence of the polarizability interaction between intense laser fields and molecules. This interaction can be used also to deflect and focus molecular beams (Seideman, 1997a, 1997b, 1997c, 1999b; Stapelfeldt *et al.*, 1997; Sakai, Tarasevitch, *et al.*, 1998; Zhao *et al.*, 2000; Chung *et al.*, 2001) and to trap (Friedrich and Herschbach, 1995a, 1995b), accelerate, and angularly accelerate (Karczmarek *et al.*, 1999; Friedrich, 2000; Villeneuve *et al.*, 2000; Barker and Schneider, 2001; Hasbani *et al.*, 2002) molecules. In much the same way that weak cw laser fields have laid the foundation to the field of atomic optics, strong laser pulses are now providing the basis of molecular optics. With this approach, the external degrees of freedom of molecules are efficiently controlled, opening the door for new applications.

ACKNOWLEDGMENTS

REFERENCES

Althorpe, S. C., and T. Seideman, 2000, J. Chem. Phys. **113**, 7901.

Andryushin, A. I., and M. V. Fedorov, 1999, JETP **89**, 837.

Aquilanti, V., D. Ascenzi, D. Cappelletti, and F. Pirani, 1994, Nature (London) **371**, 399.

Aquilanti, V., D. Ascenzi, M. de Castro Vitores, F. Pirani, and D. Cappelletti, 1999, J. Chem. Phys. **111**, 2620.

Auger, A., A. Ben Haj-Yedder, E. Cances, C. Le Bris, C. M. Dion, A. Keller, and O. Atabek, 2002, Math. Models Meth. Appl. Sci. **12**, 1281.

Averbukh, I. Sh., and R. Arvieu, 2001, Phys. Rev. Lett. **87**, 163601.

Barker, P. F., and M. N. Schneider, 2001, Phys. Rev. A **64**, 033408.

Bartels, R. A., T. C. Weinacht, N. Wagner, M. Baertschy, Chris H. Greene, M. M. Murnane, and H. C. Kapteyn, 2002, Phys. Rev. Lett. **88**, 013903.

Baugh, D. A., D. Y. Kim, V. A. Cho, L. C. Pipes, J. C. Petteway, and C. D. Fuglesang, 1994, Chem. Phys. Lett. **219**, 207.

Baumfalk, R., N. H. Nahler, and U. Buck, 2001, J. Chem. Phys. **114**, 4755.

Ben Haj-Yedder, A., A. Auger, C. M. Dion, E. Canè, A. Keller, C. Le Bris, and O. Atabek, 2002, Phys. Rev. A **66**, 063401.

Bhardwaj, V. R., D. M. Rayner, D. M. Villeneuve, and P. B. Corkum, 2001, Phys. Rev. Lett. **87**, 253003.

Blanchet, V., M. Zgierski, T. Seideman, and A. Stolow, 1999, Nature (London) **401**, 52.

Brooks, P. R., J. S. McKillop, and H. G. Pippin, 1979, Chem. Phys. Lett. **66**, 144.

Cai, L., J. Marango, and B. Friedrich, 2001, Phys. Rev. Lett. **86**, 775.

Cho, V. A., and R. B. Bernstein, 1991, J. Phys. Chem. **95**, 8129.

Chung, H. S., B. S. Zhao, S. H. Lee, S. Hwang, K. Cho, S.-H. Shim, S.-M. Lim, W. K. Kang, and D. S. Chung, 2001, J. Chem. Phys. **114**, 8293.

de Vries, M. S., V. I. Srdanov, C. P. Hanrahan, and R. M. Martin, 1983, J. Chem. Phys. **78**, 5582.

Dion, C. M., A. D. Bandrauk, O. Atabek, A. Keller, H. Umeda, and Y. Fujimura, 1999, Chem. Phys. Lett. **302**, 215.

Dion, C. M., A. Ben Haj-Yedder, E. Cances, C. Le Bris, A. Keller, and O. Atabek, 2002, Phys. Rev. A **65**, 063408.

Dietrich, P., and P. Corkum, 1992, J. Chem. Phys. **97**, 3187.

Dion, C. M., A. Keller, and O. Atabek, 2001, Eur. Phys. J. D **14**, 249.

Dion, C. M., A. Keller, O. Atabek, and A. D. Bandrauk, 1999, Phys. Rev. A **59**, 1382.

Eppink, A. T. J. B., and D. H. Parker, 1997, Rev. Sci. Instrum. **68**, 3477.

Estler, R. C., and R. N. Zare, 1978, J. Am. Chem. Soc. **100**, 1323.

Even, U., J. Jortner, D. Noy, N. Lavie, and C. Cossart-Magos, 2000, J. Chem. Phys. **112**, 8068.

Friedrich, B., 2000, Phys. Rev. A **63**, 025403.

Friedrich, B., and D. R. Herschbach, 1991, Z. Phys. D: At., Mol. Clusters **18**, 153.

Friedrich, B., and D. R. Herschbach, 1995a, Phys. Rev. Lett. **74**, 4623.

Friedrich, B., and D. R. Herschbach, 1995b, J. Phys. Chem. **99**, 15686.

Friedrich, B., and D. Herschbach, 1999, J. Phys. Chem. A **103**, 10280.

Guerin, S., L. P. Yatsenko, H. R. Jasulin, O. Faucher, and B. Lavorel, 2002, Phys. Rev. Lett. **88**, 233601.

Hasbani, R., B. Ostojic, P. R. Bunker, and M. Yu Ivanov, 2002, J. Chem. Phys. **116**, 10636.

Hayden, C. C., 2002, unpublished.

Henriksen, N. E., 1999, Chem. Phys. Lett. **312**, 196.

Hoki, K., and Y. Fujimura, 2001, Chem. Phys. **267**, 187.

Hoshina, K., K. Yamanouchi, T. Ohshima, Y. Ose, and H. Todokoro, 2002, Chem. Phys. Lett. **353**, 27.

Jortner, J., S. A. Rice, and R. M. Hochstrasser, 1969, Adv. Photochem. **7**, 149.

Kalosha, V., M. Spanner, J. Herrmann, and M. Ivanov, 2002, Phys. Rev. Lett. **88**, 103901.

Karczmarek, J., J. Wright, P. B. Corkum, and M. Ivanov, 1999, Phys. Rev. Lett. **82**, 3420.

Keller, A., C. M. Dion, and O. Atabek, 2000, Phys. Rev. A **61**, 023409.

Kim, W., and P. M. Felker, 1996, J. Chem. Phys. **104**, 1147.

Kim, W., and P. M. Felker, 1997, J. Chem. Phys. **107**, 2193.

Kim, W., and P. M. Felker, 1998, J. Chem. Phys. **108**, 6763.

Kim, B., C. P. Schick, and P. M. Weber, 1995, J. Chem. Phys. **103**, 6903.

Lappas, D. G., and J. P. Marangos, 2000, J. Phys. B **33**, 4679.

Larsen, J. J., K. Hald, N. Bjerre, H. Stapelfeldt, and T. Seideman, 2000, Phys. Rev. Lett. **85**, 2470.

Larsen, J. J., N. J. Mørkbak, J. Olesen, N. Bjerre, M. Machholm, S. R. Keiding, and H. Stapelfeldt, 1998, J. Chem. Phys. **109**, 8857.

Larsen, J. J., H. Sakai, C. P. Safvan, I. Wendt-Larsen, and H. Stapelfeldt, 1999, J. Chem. Phys. **111**, 7774.

Larsen, J. J., I. Wendt-Larsen, and H. Stapelfeldt, 1999, Phys. Rev. Lett. **83**, 1123.

Legare, F., and A. D. Bandrauk, 2001, Phys. Rev. A **64**, 031406.

Legare, F., S. Chelkowski, and A. D. Bandrauk, 2000, Chem. Phys. Lett. **329**, 469.

Loesch, H. J., and J. Remscheid, 1990, J. Chem. Phys. **93**, 4779.

Machholm, M., 2001, J. Chem. Phys. **115**, 10724.

Machholm, M., and N. E. Henriksen, 2001, Phys. Rev. Lett. **87**, 193001.

Ortigoso, J., M. Rodriguez, M. Gupta, and B. Friedrich, 1999, J. Chem. Phys. **110**, 3870.

Pershan, P. S., J. P. van der Ziel, and L. D. Malmstrom, 1966, Phys. Rev. **143**, 574.

Pirani, F., D. Cappelletti, M. Bartolomei, V. Aquilanti, M. Scotoni, M. Vescovi, D. Ascenzi, and D. Bassi, 2001, Phys. Rev. Lett. **86**, 5035.

Poulsen, M. D., E. Skovsen, and H. Stapelfeldt, 2002, J. Chem. Phys. **117**, 2097.

Pullmann, D. P., B. Friedrich, and D. R. Herschbach, 1990, J. Chem. Phys. **93**, 3224.

Radloff, W., V. Stert, Th. Freudenberg, I. V. Hertel, C. Jouvet, C. Dedonder-Lardeux, and D. Solgadi, 1997, Chem. Phys. Lett. **281**, 20.

Rosca-Pruna, F., and M. J. J. Vrakking, 2001, Phys. Rev. Lett. **87**, 153902.

Rosca-Pruna, F., and M. J. J. Vrakking, 2002a, J. Chem. Phys. **116**, 6567.

Rosca-Pruna, F., and M. J. J. Vrakking, 2002b, J. Chem. Phys. **116**, 6579.

Sakai, H., S. Minemoto, H. Nanjo, H. Tanji, and T. Suzuki, 2003, Phys. Rev. Lett. **90**, 083001.

Sakai, H., C. P. Safvan, J. J. Larsen, K. M. Hilligsøe, K. Hald, and H. Stapelfeldt, 1998, J. Chem. Phys. **110**, 10235.

Sakai, H., A. Tarasevitch, J. Danilov, H. Stapelfeldt, R. W. Yip, C. Ellert, E. Constant, and P. B. Corkum, 1998, Phys. Rev. A **79**, 2794.

Seel, M., and W. Domcke, 1991, J. Chem. Phys. **95**, 7806.

Seideman, T., 1995a, J. Chem. Phys. **102**, 6487.

Seideman, T., 1995b, J. Chem. Phys. **103**, 7887.

Seideman, T., 1996, Chem. Phys. Lett. **253**, 279.

Seideman, T., 1997a, Phys. Rev. A **56**, R17.

Seideman, T., 1997b, J. Chem. Phys. **106**, 2881.

Seideman, T., 1997c, J. Chem. Phys. **107**, 10420.

Seideman, T., 1999a, Phys. Rev. Lett. **83**, 4971.

Seideman, T., 1999b, J. Chem. Phys. **111**, 4397.

Seideman, T., 2000, J. Chem. Phys. **113**, 1677.

Seideman, T., 2001a, J. Chem. Phys. **115**, 5965.

Seideman, T., 2001b, Phys. Rev. A **64**, 042504.

Seideman, T., 2002, Annu. Rev. Phys. Chem. **53**, 41.

Stapelfeldt, H., H. Sakai, E. Constant, and P. B. Corkum, 1997, Phys. Rev. Lett. **79**, 2787.

Stolow, A., 2002, private communication.

Stolte, S., 1988, in *Atomic and Molecular Beam Methods*, edited by G. Scoles (Oxford University, New York), p. 631.

Sugita, A., M. Mashino, M. Kawasaki, Y. Matsumi, N. Toyokawa, R. J. Gordon, and R. Bersohn, 2000, J. Chem. Phys. **112**, 2164.

Sugita, A., K. Suto, M. Kawasaki, and Y. Matsumi, 2001, Chem. Phys. Lett. **340**, 83.

Sukharev, M. E., and V. P. Krainov, 1998, JETP **86**, 318.

Suzuki, Y., M. Stener, and T. Seideman, 2002, Phys. Rev. Lett. **89**, 233002.

Torres, E. A., D. Y. Kim, L. C. Pipes, D. A. Baugh, and T. Seideman, 1997, J. Chem. Soc., Faraday Trans. **93**, 931.

Van Leuven, P., M. Malvaldi, and M. Persico, 2002, J. Chem. Phys. **116**, 538.

Velotta, R., N. Hay, M. B. Mason, M. Castillejo, and J. P. Marangos, 2001, Phys. Rev. Lett. **87**, 183901.

Villeneuve, D., S. A. Aseyev, P. Dietrich, M. Spanner, M. Yu Ivanov, and P. B. Corkum, 2000, Phys. Rev. Lett. **85**, 542 (2000).

Weida, M. J., and C. S. Parmenter, 1997, J. Chem. Phys. **107**, 7138.

Wu, M., R. J. Bemish, and R. E. Miller, 1994, J. Chem. Phys. **101**, 9447.

Yan, Z.-C., and T. Seideman, 1999, J. Chem. Phys. **111**, 4113.

Zare, R. N., 1988, *Angular Momentum* (Wiley, New York).

Zhao, B. S., *et al.*, 2000, Phys. Rev. Lett. **85**, 2705.

Zon, B. A., and B. G. Katsnel'son, 1976, Sov. Phys. JETP **42**, 595.